Available online at www.sciencedirect.com

ScienceDirect

Journal of the European Ceramic Society 34 (2014) 3627–3633

www.elsevier.com/locate/jeurceramsoc

High-strength AlN ceramics by low-temperature sintering with $CaZrO_3$–Y_2O_3 co-additives

Hyun Min Lee, Do Kyung Kim *

Department of Materials Science and Engineering, Korea Advanced Institute of Science and Technology (KAIST), 291 Daehak-ro, Yuseong-gu, Daejeon 305-701, Republic of Korea

Received 5 March 2014; received in revised form 3 May 2014; accepted 5 May 2014
Available online 2 June 2014

Abstract

Aluminum nitride (AlN) ceramics with the concurrent addition of $CaZrO_3$ and Y_2O_3 were sintered at 1450-1700 °C. The degree of densification, microstructure, flexural strength, and thermal conductivity of the resulting ceramics were evaluated with respect to their composition and sintering temperature. Specimens prepared using both additives could be sintered to almost full density at relatively low temperature (3 h at 1550 °C under nitrogen at ambient pressure); grain growth was suppressed by grain-boundary pinning, and high flexural strength over 630 MPa could be obtained. With two-step sintering process, the morphology of second phase was changed from interconnected structure to isolated structure; this two-step process limited grain growth and increased thermal conductivity. The highest thermal conductivity (156 $Wm^{-1} K^{-1}$) was achieved by two-step sintering, and the ceramic showed moderate flexural strength (560 MPa).

Keywords: Aluminum nitride; $CaZrO_3$; Strength; Thermal conductivity; Sintering

1. Introduction

Aluminum nitride (AlN) is a useful ceramic material for many technical applications like substrate, heat sinks, refractive materials in metallurgical industry, packaging materials for high power integrated circuits for electronic devices, due to its combination of high thermal conductivity, low dielectric constant, high electrical resistance, wide band gap ($E_g = 6.2$ eV at room temperature), chemical inertness, and thermal expansion coefficient (which is close to that of silicon).[1–6] The thermal conductivity of AlN and the factors affected by it have received much attention for several decades.[7–10] The high power-density required in many applications can cause crack propagation in ceramic substrates owing to high thermal stresses arising at the joints with circuits. Therefore, for AlN ceramics to be widely useful, they must show high thermal conductivity and good mechanical properties. A few studies have focused on the mechanical properties of AlN. Watari and Hwang investigated the thermal conductivity and flexural strength of $LiYO_2$–CaO-doped AlN ceramics,[11] finding respective values of 170 $Wm^{-1} K^{-1}$ and 440 MPa. They concluded that both properties were influenced by AlN grain size and the number of grain boundaries.

The flexural strength of AlN ceramics can be improved by eliminating pores and by having smaller grains. However, decreasing the grain size reduces the thermal conductivity of the sintered material. Therefore, new fabrication techniques are sought that produce ceramic substrates with high thermal conductivity and good mechanical properties.

The primary objective of this work is the fabrication of AlN ceramics with both high flexural strength and high thermal conductivity. The AlN ceramics were pressureless sintered at 1450–1700 °C for 3 h with $CaZrO_3$ and Y_2O_3 additives. CaO–Y_2O_3 is the most popular additive system for the low-temperature sintering of AlN ceramics due to its low eutectic temperature.[12,13] However, large grains tend to form in the resulting sintered AlN, leading to poor flexural strength. The inhibition of grain growth is therefore desirable, because it would lead to smaller grains and stronger ceramics. Secondary phase inclusions can inhibit grain growth, and are frequently used for this purpose in sintered ceramics. Lange and Hirlinger used ZrO_2

* Corresponding author. Tel.: +82 42 350 4118; fax: +82 42 350 3310.
E-mail address: dkkim@kaist.ac.kr (D.K. Kim).

http://dx.doi.org/10.1016/j.jeurceramsoc.2014.05.008
0955-2219/

to inhibit grain growth for Al_2O_3 sintering.[14,15] The secondary phases were located at the grain boundaries and they hindered grain growth by exerting a dragging force and by pinning the grain boundary.[14]

$CaZrO_3$ is a phase between CaO–ZrO_2 that is stable at high temperature.[16] This sintering additive plays a double role during the sintering process. One is to promote the densification by forming a liquid phase when it is in contact with Al_2O_3 in presence of certain impurities. Mostly, AlN raw powder contains a small amount of oxygen impurity which is Al_2O_3 existed on the surface of AlN. The other is to suppress grain growth, keeping the grains small via grain-boundary pinning from the secondary phase. The resulting small grains can yield AlN ceramics with high flexural strength. The addition of CaO can also promote the secondary phase to be located at the boundaries of the AlN grains during sintering.[17]

Sintering in two-steps can produce AlN ceramics that are both strong and highly thermal conductive.[18,19] Chen and Wang introduced this technique to suppress grain growth during the final stage of sintering.[19] The thermal conductivity of AlN ceramics is affected by phonon-defect scattering caused by oxygen-related defects and secondary phases.

This work reports the two-step sintering of AlN ceramics with $CaZrO_3$ and Y_2O_3 additives. The additives suppressed grain growth, and the two-step sintering process provided high thermal conductivity without reducing flexural strength. The second step of the sintering was conducted at temperatures that allowed active grain boundary diffusion but hindered grain boundary migration. Consequently, densification and purification of the AlN lattice were able to continue without significant grain growth.[20,21]

2. Experimental procedure

2.1. Powders and processing

Green AlN specimens were prepared using commercial high-purity AlN power (particle size 1.0 μm, specific surface area 3.27 $m^2\,g^{-1}$; E grade, Tokuyama Corp., Tokyo, Japan) with additives of $CaZrO_3$ (particle size <50 nm, Aldrich, USA) and Y_2O_3 (particle size 30 nm, Aldrich, USA). Three systems employing both additives were tested: both additives were each used at 1 wt. % (system CzY), 2 wt. % (Cz2Y2), and 3 wt. % (Cz3Y3). The AlN powder and the additives were ball milled using zirconia balls for 24 h in a polyethylene bottle with 2-propanol as liquid medium. After mixing, the slurry was dried on a hot plate with stirring. The dried powder was sieved through a 100-mesh sieve and then shaped into 20 mm diameter disk under a pressure of 30 $kg\,cm^{-2}$, and was cold isostatic pressed (CIP) at 200 MPa. A similarly prepared system of only Y_2O_3-doped AlN (system Y) was also tested for comparison.

2.2. Sintering

All the systems were sintered using both one-step and two-step regimes. The green bodies shaped through CIP were sintered between two boron nitride (BN) plates. Sintering was at 1450–1700 °C for 3 h under a nitrogen atmosphere in a graphite furnace (ASTRO, Thermal Technology, Santa Barbara, CA). The heating rate during sintering was 10 °C/min; the cooling rate was 25 °C/min.

Two-step sintering was conducted using different temperatures to minimize grain growth. The second sintering temperature was selected to promote densification and purification of the AlN lattice without allowing grain growth. During the first step, specimens were heated to T_1 with rate of 10 °C/min and held for 3 h at T_1. They were cooled at 25 °C/min to a lower sintering temperature T_2, which was then maintained for 2 h.

2.3. Characterization

Bulk density was measured by Archimedes' method. The microstructure of facture surfaces and the mean diameter of the grains were characterized by scanning electron microscopy (FE-SEM; Philips XL30 FEG, Eindhoven, Netherlands) and transmission electron microscopy (TEM; Tecnai G^2 F30 S-twin FEI, Eindhoven, The Netherlands). The thermal conductivity at room temperature was measured by the laser flash method with a glass–Nd laser and an InSb infrared sensor using a Xenon Flash instrument (LFA 447 Nanoflash, Netzsch Instruments Inc., Burlington, USA).[22] The precision of this apparatus is estimated to be ±3 %. Each reported thermal conductivity is an average of three measurements.

The flexural strength of 1.5 mm × 2.0 mm × 15 mm rectangular bars was tested using a 10 mm support span and a crosshead speed of 0.2 mm/min. Sintered disks were cut into bars for the measurements. The bars were polished with 6 μm diamond paste in alcohol-based slurry (Blue Lube, Struers) and flaws on either side of each bar were removed. The reported flexural strength is an average of the test results of ten bending bars.

3. Result and discussion

3.1. Densification behavior

The AlN ceramics sintered with various additive concentrations showed bulk density values that depended on the sintering temperature (Fig. 1). The green densities of the powder compacts were approximately 57–60 % of theoretical density (TD). The density of each specimen increased as the sintering temperature increased from room temperature to 1550 °C. The theoretical density of AlN was reached by each sample, with the exception of sample Y, when sintered at over 1550 °C. Sample Y, which lacked $CaZrO_3$, achieved only 81 % of the TD after sintering at 1550 °C for 3 h (Fig. 1). Overall, the bulk density comparison shows that the use of both $CaZrO_3$ and Y_2O_3 additives greatly improved the sinterability of AlN ceramics and achieved the lower temperature sintering process. The densification was achieved by means of liquid-phase sintering. The $CaZrO_3$–Y_2O_3–Al_2O_3 additive system formed a liquid phase by eutectic melting, which promoted densification at lower temperatures.

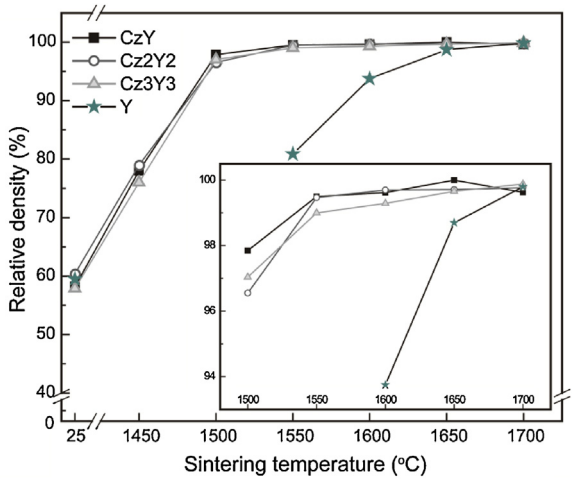

Fig. 1. Relative density of AlN ceramics sintered at various temperatures for 3 h.

Table 1
Flexural strength of AlN sintered at various temperatures.

Temperature (°C)	Flexural strength[a] (MPa)		
	CzY	CzY2	CzY3
1500	579 (60)	540 (82)	456 (48)
1550	539 (39)	631 (52)	515 (34)
1600	568 (63)	562 (34)	568 (41)
1650	517 (19)	516 (36)	596 (62)
1700	506 (44)	472 (35)	462 (17)

[a] Standard deviations for ten measurements given in parentheses.

3.2. Flexural strength of AlN

A three-point bending test was conducted on each of the AlN ceramics with two additives after sintering at 1500, 1550, 1600, 1650, and 1700 °C (Table 1 and Fig. 2). Specimens sintered at 1450 °C were not sufficiently dense to warrant strength assessment. Ten samples of each composition were tested at each temperature. Strengths of over 450 MPa were consistently observed at all the tested sintering temperatures. Among the three tested compositions, Cz2Y2 had the highest flexural strength of 630 MPa after sintering at 1550 °C. The flexural strength of this composition initially increased with sintering temperature increased, but it then decreased as the sintering temperature increased above a certain optimal temperature due to the increased promotion of grain growth. The measured strengths of the various compositions showed different trends with respect to sintering temperature. As the amount of additives increased, the sintering temperature required to achieve the highest strength was raised. Sample CzY showed its the highest flexural strength after sintering at 1500 °C, Cz2Y2 was the strongest after sintering at 1550 °C, and Cz3Y3 after sintering at 1650 °C.

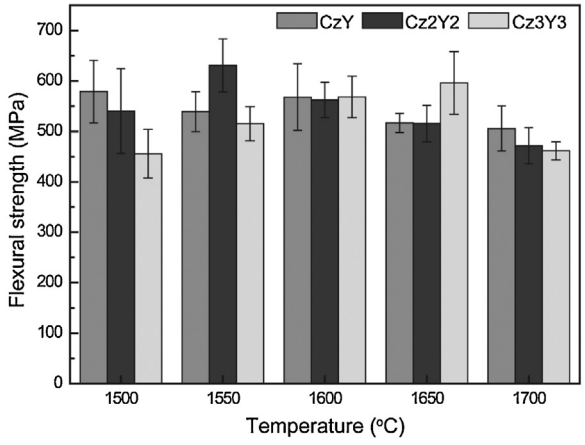

Fig. 2. Flexural strength of AlN ceramics sintered at various temperatures.

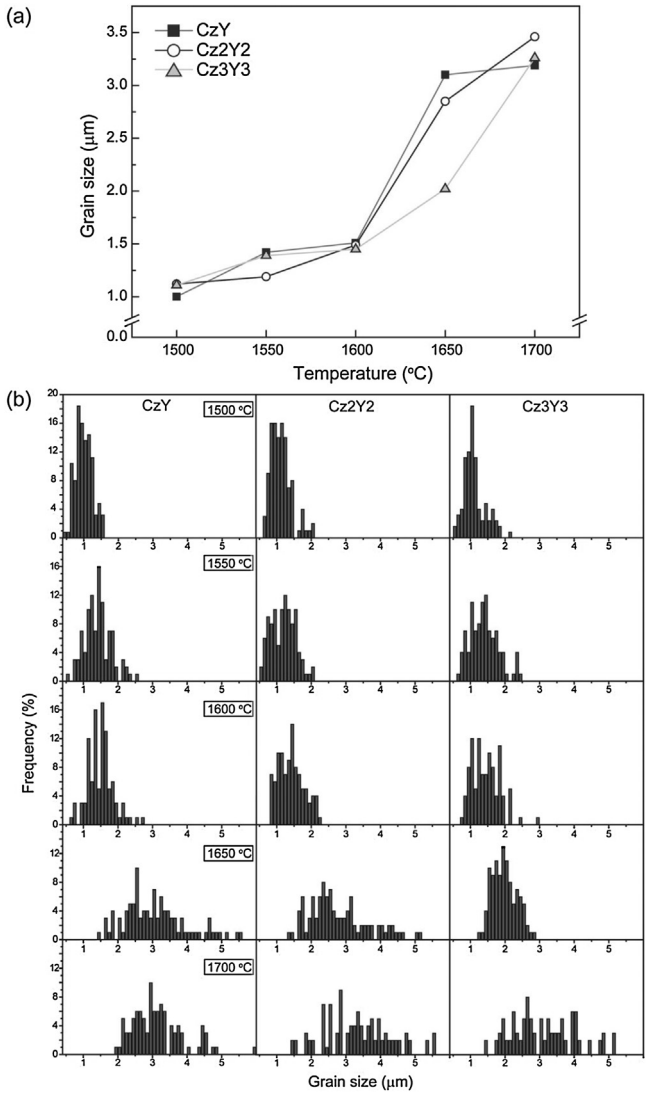

Fig. 3. (a) Grain size of AlN ceramics sintered at various temperatures. (b) Grain size distribution of CzY, Cz2Y2, and Cz3Y3 compositions.

The flexural strength of a specimen is generally affected by its pores and grain size. However, all three compositions showed full densification after sintering at over 1500 °C with no pores inside the lattices. The increased addition of $CaZrO_3$ effectively limited grain growth, even during sintering at high temperatures. Fig. 3 shows grain size distributions for the various combinations of sintering temperature and composition. The samples with the smallest grains showed the highest flexural strengths

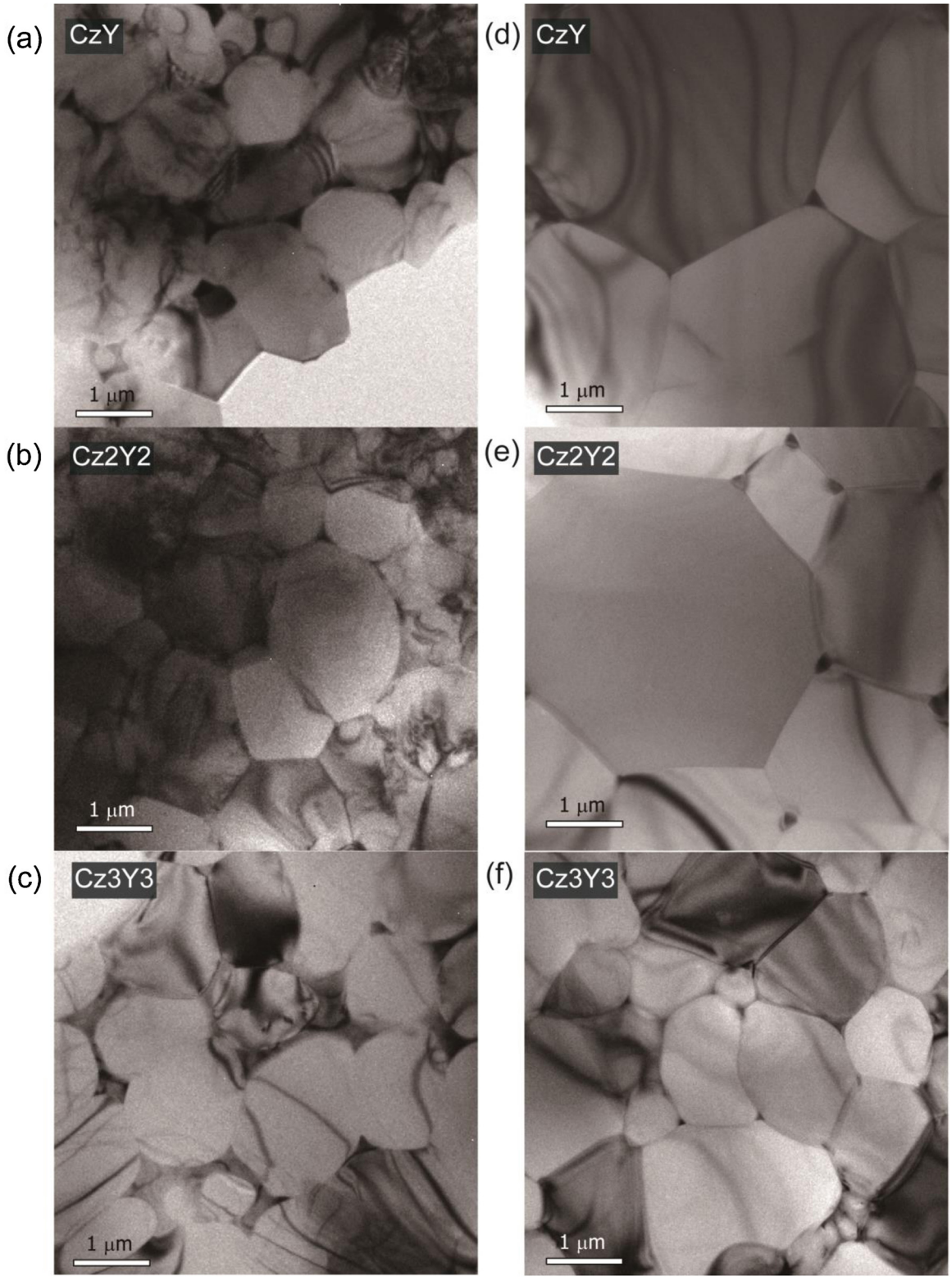

Fig. 4. TEM images of (a) CzY, (b) Cz2Y2, (c) Cz3Y3 compositions sintered at 1650 °C.

(Figs. 2 and 3). CzY showed the highest strength and the smallest grains among the three compositions after each was sintered at 1500 °C. Sintering at 1550 °C left Cz2Y2 the strongest ceramic with the smallest grains; Cz3Y3 was the strongest and finest grained of the samples sintered at 1650 °C. Higher additive concentrations maintained small grains in the ceramics sintered at high temperature (1650 °C). Small amount of $CaZrO_3$ additives formed liquid phase by reacting with Al_2O_3 in advance and the remaining $CaZrO_3$ could inhibit the grain growth by locating at the triple junctions of grains.

The grains of Cz3Y3, the sample with the highest additive concentration, were limited to being 2 μm in size when the sample was sintered at up to 1650 °C. They also showed a narrow distribution of sizes. On the other hand, the grains of CzY and Cz2Y2 showed the grain growth. In both CzY and Cz2Y2 compositions, added small amount of $CaZrO_3$ additives had less effect on inhibiting the grain growth at high temperature, because $CaZrO_3$ reacted with Al_2O_3 and formed liquid phase. Grain properties tend to affect significantly the strength of the ceramics, with strong materials showing narrow distributions of small grains, as also observed in the ceramics studied here (Figs. 2 and 3).

3.3. Microstructure analysis

Transmission electron microscopy (TEM) analysis of the sintered specimens was conducted to compare the characteristics of their various grains. In Fig. 4(a)–(c) microstructure of AlN sintered at 1600 °C showed similar morphology and grain size. Cz3Y3 showed small, rounded grains in sintered at 1650 °C, while CzY and Cz2Y2 showed large, faceted grains (Fig. 4(d)–(f)). The small grains of Cz3Y3 appeared to exhibit grain-boundary pinning with a secondary phase at the triple junctions among them (Figs. 4 and 5). STEM (scanning transmission electron microscope) and elemental mapping analyses of Cz3Y3 sintered at 1650 °C revealed that the secondary phase was separated into two regions, one brighter than the other (respectively labeled 1 and 2 in Fig. 5(a)). The brighter region at the triple junctions among the grains contained a 1:1 ratio of calcium and zirconium elements, suggesting that the added $CaZrO_3$ was present at these junctions and provided the pinning force at the grain boundaries. Fig. 5(b) also shows zirconium located mainly in the brighter region. The added Y_2O_3 and a small amount of CaO, which was derived from the added $CaZrO_3$, reacted with Al_2O_3 from the surface oxide layer of the AlN to form a liquid phase that prevented the diffusion of oxygen into the grains by trapping it at the grain boundaries. The sintering additives affected the grain properties of the ceramics via two separate processes: grain-boundary pinning and the elimination of oxygen-related defects (Fig. 5). These processes allowed grain growth and flexural strength to be controlled by the addition of $CaZrO_3$ and Y_2O_3. The use of the additives enabled the ceramics to have smaller grains than otherwise observed under similar sintering conditions.

3.4. Enhancement of thermal conductivity by two-step sintering

The use of the additives strengthened the AlN ceramics, and subsequent elaboration of the sintering process (i.e., two-step sintering), further enhanced their thermal conductivity without compromising their strength. Fig. 6 compares the thermal conductivities and flexural strengths of the AlN ceramics sintered at 1600 °C and at two-step temperatures (1600 °C and then 1400 °C). The one-step sintering resulted in thermal conductivities for CzY, Cz2Y2, and Cz3Y3 of 120, 132, and 144 $Wm^{-1} K^{-1}$, respectively. The two-step sintered ceramics

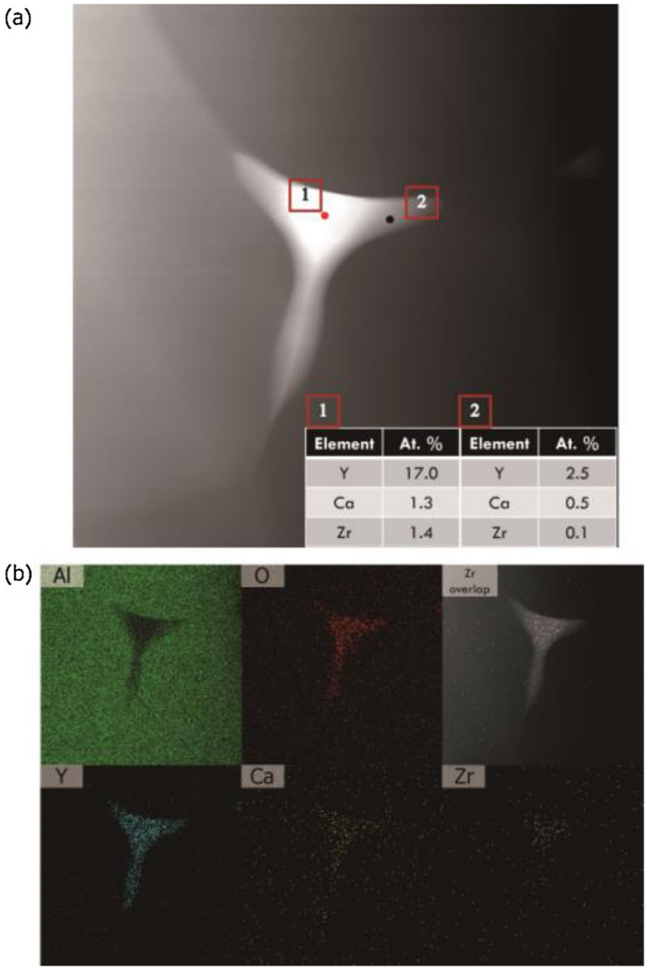

Fig. 5. (a) STEM micrograph and (b) elemental mapping analysis of Cz3Y3 ceramics sintered at 1650 °C. The secondary phase shows two regions: a brighter region (labeled 1) located at the triple junction of grains, which contains a 1:1 ratio of calcium and zirconium elements, and a less bright region (labeled 2). Zirconium is mostly located in the brighter region.

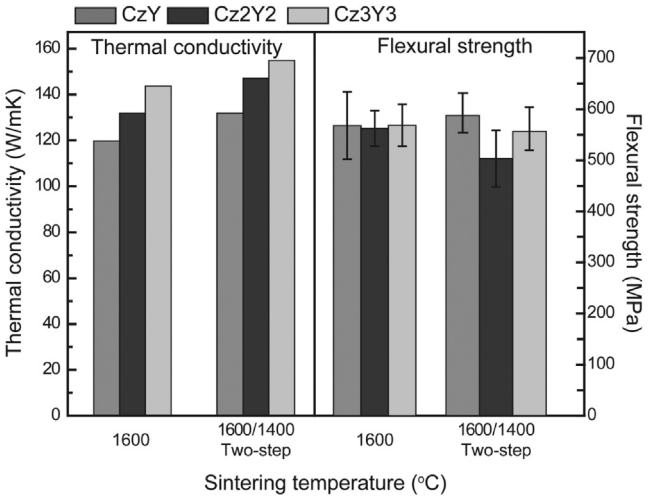

Fig. 6. Thermal conductivity and flexural strength of specimens sintered by one- and two-step process.

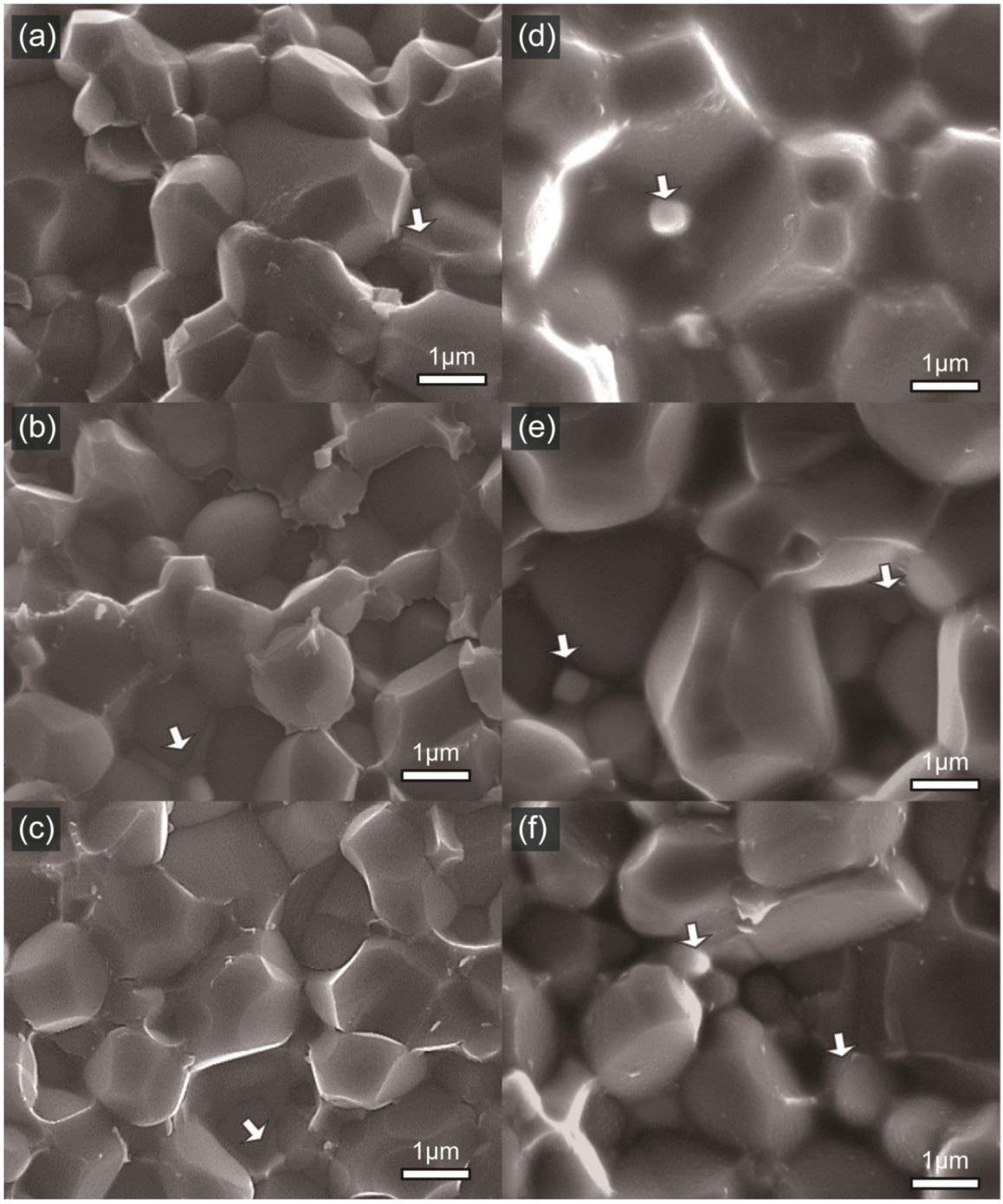

Fig. 7. Microstructure of (a, d) CzY, (b, e) Cz2Y2, and (c, f) Cz3Y3 compositions: arrows indicate the second phase. One-step sintered specimens show a channel-like structure of the second phase (a, b, c). Two-step sintered specimens show an isolated second phase at the triple junction of the grains (d, e, f).

were on average 9.7 % more thermally conductive: their respective thermal conductivities were 132, 147, and 155 $Wm^{-1} K^{-1}$. The flexural strengths and grain sizes of the variously sintered ceramics are compared in Table 2. Two-step sintering led to grains on average 12.6 % larger than those resulting from one-step sintering; though the longer holding time of two-step sintering process showed a minimal grain growth, it did not greatly affect both thermal conductivity and strength. The microstructures of the one- and two-step sintered samples are compared in Fig. 7. Sintering at one temperature resulted in

Table 2
Flexural strength and grain size of AlN sintered in one (1600 °C) or two steps (1600/1400 °C).

Composition	Strength[a] (MPa)		Grain size (μm)	
	One-step	Two-step	One-step	Two-step
CzY	568 (60)	592 (39)	1.51	1.61
Cz2Y2	562 (82)	501 (55)	1.49	1.74
Cz3Y3	568 (48)	560 (42)	1.45	1.66

[a] Standard deviations for ten measurements given in parentheses.

a secondary phase along the grain boundaries that formed a continuous channel-like structure (Fig. 7(a)–(c)); in the two-step sintered samples, the secondary phase was isolated at the triple junctions of the grains (Fig. 7(d)–(f)). Such an isolated secondary phase led to reduced phonon-defect scattering, suggesting that the difference in the morphologies of the secondary phase was the main cause of the different thermal conductivities observed here. The isolated secondary phase resulted in enhanced thermal conductivity.

4. Conclusions

This work has demonstrated that the low-temperature (1550 °C) sintering of AlN with $CaZrO_3$ and Y_2O_3 additives resulted in dense ceramics that approached the theoretical density. The $CaZrO_3$–Y_2O_3 additive system allowed low temperature sintering to produce high-strength AlN materials. The additives limited the grain size to 2 μm in AlN ceramics sintered at up to 1650 °C. They also suppressed grain growth during high temperature sintering through grain-boundary pinning. As the amount of additives increased, the sintering temperature required to achieve the highest strength was raised. $CaZrO_3$ and Y_2O_3 additives, each used at 1 wt. %, led to a ceramic with an optimized flexural strength of 579 MPa obtained after sintering at 1500 °C. The additives used at 2 wt. % resulted in an optimized strength of 631 MPa with sintering at 1550 °C, and flexural strength was maximized at 596 MPa in a system with 3 wt. % of each additive sintered at 1650 °C. The thermal conductivities of the AlN ceramics were enhanced by using a two-step sintering process; this did not weaken the ceramics. Phonon-defect scattering related to secondary phases decreased with the introduction of isolated secondary phases during the two-step processing. The highest thermal conductivity shown by the AlN ceramics was 156 $Wm^{-1} K^{-1}$, the flexural strength of this two-step-sintered sample was 560 MPa.

Acknowledgments

This study was supported by a grant from the Fundamental R&D Program for Core Technology of Materials funded by the Ministry of Commerce, Industry and Energy, Republic of Korea. This work was also supported by the Basic Science Research Program through the National Research Foundation of Korea (NRF) funded by the Ministry of Education (2009-0094038). The authors wish to express their gratitude to Dr. In-Sig Seog of KCC for his valuble suggestion and support durig this study.

References

1. Slack GA, Tanzilli RA, Pohl RO, Vandersande JW. The intrinsic thermal conductivity of AlN. *J Phys Chem Solids* 1987;**48**:641–7.
2. Bachelard R, Joubert P. Aluminum nitride by carbothermal reduction. *Mater Sci Eng A* 1989;**109**:247–51.
3. Sheppard LM. Aluminum nitride: a versatile but challenging material. *Am Ceram Soc Bull* 1990;**69**(11):1801–10.
4. Watanabe M, Mori Y, Ishikawa T, Iida T, Akiyama K, Sawabe K, et al. X-ray photoelectron spectroscopy of polycrystalline AlN surface exposed to the reactive environment of XeF_2. *Appl Surf Sci* 2003;**217**(1–4):82–7.
5. Chouanine L, Takano M, Ashihara F, Kamiya O. Influence of the surface topography on the micromechanical properties and performance of a CMP finished AIN component for silicon plasma etching. *Adv Fract Fail Prev* 2004;**261–263**(Pts 1 and 2):1599–604.
6. Kume S, Yasuoka M, Omura N, Watari K. Effects of annealing on dielectric loss and microstructure of aluminum nitride ceramics. *J Am Ceram Soc* 2005;**88**(11):3229–31.
7. Kim WJ, Kim DK, Kim CH. Morphological effect of second phase on the thermal conductivity of AlN ceramics. *J Am Ceram Soc* 1996;**79**(4):1066–72.
8. Watari K, Ishizaki K. Thermal conduction mechanism of aluminum nitride ceramics. *J Mate Sci* 1992;**27**:2627–30.
9. Kurokawa Y, Utsumi K, Takamizawa H. Development and microstructural characterization of high-thermal-conductivity aluminum nitride ceramics. *J Am Ceram Soc* 1988;**71**(7):588–94.
10. Lee HK, Kim DK. Defect characterization of high thermal conductivity CaF_2 doped AlN ceramics by Raman spectroscopy. *Mod Phys Lett B* 2009;**23**(31–32):3869–76.
11. Watari K, Hwang HJ, Toriyama M, Kanzaki S. Effective sintering aids for low-temperature sintering of AlN ceramics. *J Mater Res* 1999;**14**(4):1409–17.
12. Qiu JY, Hotta Y, Watari K, Mitsuishi K, Yamazaki M. Low-temperature sintering behavior of the nano-sized AlN powder achieved by superfine grinding mill with Y_2O_3 and CaO additives. *J Eur Ceram Soc* 2006;**26**(4–5):385–90.
13. Chu CH, Lin CP, Wen SB, Shen YH. Sintering of aluminum nitride by using alumina crucible and $MoSi_2$ heating element at temperatures of 1650 degrees C and 1700 degrees C. *Ceram Int* 2009;**35**(8):3455–61.
14. Lange FF, Hirlinger MM. Hindrance of grain-growth in Al_2O_3 by ZrO_2 inclusions. *J Am Ceram Soc* 1984;**67**(3):164–8.
15. Xue LA, Meyer K, Chen IW. Control of grain-boundary pinning in Al_2O_3/ZrO_2 Composites with Ce^{3+}/Ce^{4+} doping. *J Am Ceram Soc* 1992;**75**(4):822–9.
16. Nishino T. Estimation of a portion of phase-diagram in CaO–ZrO_2 system by reacting $CaZrO_3$ with Cr_2O_3. *Nippon Kagaku Kaishi* 1981;**10**:1681–3.
17. Surnev S, Lepkova D, Yoleva A. Influence of the sintering additives on the phase-composition and the thermal-conductivity of aluminum nitride ceramics. *Mater Sci Eng B* 1991;**10**(1):35–40.
18. Mazaheri M, Zahedi AM, Hejazi MM. Processing of nanocrystalline 8 mol % yttria-stabilized zirconia by conventional, microwave-assisted and two-step sintering. *Mater Sci Eng A* 2008;**492**(1–2):261–7.
19. Mazaheri M, Haghighatzadeh M, Zahedi AM, Sadrnezhaad SK. Effect of a novel sintering process on mechanical properties of hydroxyapatite ceramics. *J Alloys Compd* 2009;**471**(1–2):180–4.
20. Chen IW, Wang XH. Sintering dense nanocrystalline ceramics without final-stage grain growth. *Nature* 2000;**404**(6774):168–71.
21. Hesabi ZR, Haghighatzadeh A, Mazaheri M, Galusek D, Sadrnezhaad SK. Suppression of grain growth in sub-micrometer alumina via two-step sintering method. *J Eur Ceram Soc* 2009;**29**(8):1371–7.
22. Murabaya M, Takahash Y, Mukaibo T. Measurement of heat capacity at high temperatures by laser flash method – heat capacity of alumina. *J Nucl Sci Technol* 1970;**7**(6):312–20.